



Neural stem cell differentiation by electrical stimulation using a cross-linked PEDOT substrate: Expanding the use of biocompatible conjugated conductive polymers for neural tissue engineering



Filipa Pires^{a,b,c}, Quirina Ferreira^a, Carlos A.V. Rodrigues^{b,c}, Jorge Morgado^{a,b,*}, Frederico Castelo Ferreira^{b,c,**}

^a Instituto de Telecomunicações, Av. Rovisco Pais, 1049-001 Lisboa, Portugal

^b Department of Bioengineering, Instituto Superior Técnico, Universidade de Lisboa, Av. Rovisco Pais, 1049-001 Lisboa, Portugal

^c iBB-Institute for Bioengineering and Biosciences, Instituto Superior Técnico, Universidade de Lisboa, Av. Rovisco Pais, 1049-001 Lisboa, Portugal

ARTICLE INFO

Article history:

Received 5 December 2014

Received in revised form 24 January 2015

Accepted 30 January 2015

Available online 7 February 2015

Keywords:

Conjugated conductive polymer

Cross-linked PEDOT:PSS

Electrical stimulation

Human neural stem cell

Neuron

ABSTRACT

Background: The use of conjugated polymers allows versatile interactions between cells and flexible processable materials, while providing a platform for electrical stimulation, which is particularly relevant when targeting differentiation of neural stem cells and further application for therapy or drug screening.

Methods: Materials were tested for cytotoxicity following the ISO10993-5. PEDOT:PSS was cross-linked. ReNcellVM neural stem cells (NSC) were seeded in laminin coated surfaces, cultured for 4 days in the presence of EGF (20 ng/mL), FGF-2 (20 ng/mL) and B27 (20 µg/mL) and differentiated over eight additional days in the absence of those factors under 100 Hz pulsed DC electrical stimulation, 1 V with 10 ms pulses. NSC and neuron elongation aspect ratio as well as neurite length were assessed using ImageJ. Cells were immune-stained for Tuj1 and GFAP.

Results: F8T2, MEH-PPV, P3HT and cross-linked PEDOT:PSS (xPEDOT:PSS) were assessed as non-cytotoxic. L929 fibroblast population was 1.3 higher for xPEDOT:PSS than for glass control, while F8T2 presents moderate proliferation. The population of neurons (Tuj1) was 1.6 times higher with longer neurites (73 vs 108 µm) for cells cultured under electrical stimulus, with cultured NSC. Such stimulus led also to longer neurons.

Conclusions: xPEDOT:PSS was, for the first time, used to elongate human NSC through the application of pulsed current, impacting on their differentiation towards neurons and contributing to longer neurites.

General Significance: The range of conductive conjugated polymers known as non-cytotoxic was expanded. xPEDOT:PSS was introduced as a stable material, easily processed from solution, to interface with biological systems, in particular NSC, without the need of in-situ polymerization.

© 2015 Elsevier B.V. All rights reserved.

1. Introduction

The use of conjugated polymers allows versatile interactions between cells and flexible processable materials that promote cell adhesion along with electrical stimulation [1–3]. The use of such materials in combination with cells has a high potential when considering smart electron interfaces, neuroprosthetic devices, neural probes, cell-electrical studies, drug delivery and, more recently, in the context of regenerative medicine. Conjugated polymers can be used to build scaffolds to support cells, while providing electrical stimulus. This is particularly relevant when targeting differentiation of neural stem

cells, into neurons and glial cells, and further application for novel regenerative therapies, for neural degenerative diseases and spinal cord injuries, or drug discovery and neural toxicity testing [4–6].

Within this context, conductive conjugated polymers, whose backbone is made of alternating double- and single-bonds [3], have earned attention as they respond to light and electrical stimuli and their molecular structure can be tuned to minimize toxic effects [3,7,8]. Polypyrrole (PPy), polyaniline (PANI), poly(3,4-ethylenedioxythiophene):polystyrene sulfonate (PEDOT:PSS), poly(3-hexylthiophene) (P3HT) and poly(2,2'-bithiophene) (PBP) are among the conjugated polymers already used with mammalian cell system that exhibit an acceptable biocompatibility [9–14].

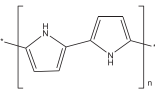
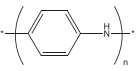
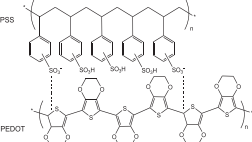
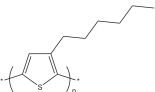
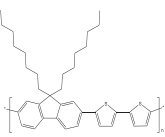
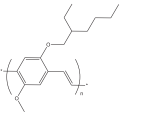
PPy and PEDOT:PSS are among the conjugated polymers with higher conductivity [15]. The range of conjugated polymers assessed as cell scaffold supports is actually fairly limited. A non-comprehensive summary of such studies is provided in Table 1. Whereas, many of the studies are focused on exploring the ability of these polymers to mobilize proteins and promote cell adhesion in different fashions and studying the effects on cell fate on the absence of external electric

* Correspondence to: Department of Bioengineering and Instituto de Telecomunicações, Instituto Superior Técnico, Universidade de Lisboa, Av. Rovisco Pais, 1049-001 Lisboa, Portugal. Tel.: +351 218418451.

** Correspondence to: Department of Bioengineering and IBB-Institute for Bioengineering and Biosciences, Instituto Superior Técnico, Universidade de Lisboa, Av. Rovisco Pais, 1049-001 Lisboa, Portugal. Tel.: +351 218419598.

E-mail addresses: jmfmorgado@tecnico.ulisboa.pt (J. Morgado), frederico.ferreira@tecnico.ulisboa.pt, fredericocastelo@yahoo.com (F.C. Ferreira).

Table 1
Brief summary of conjugated polymers used in this and previous works.

Conjugated polymer	Chemical structure	Previous work	Our work
Poly pyrrole (PPy)		<ul style="list-style-type: none"> Extensively used with mammalian cells Electric stimulation of human neural stem cells, rat neural explants, PC-12 cells [47–50] Modulation of survival and maintenance of rat fetal neural stem and human embryonic stem cells [22], mesenchymal cells [21,51] Scaffolds containing stimuli to enhance tissue regeneration [9,23,52,53] 	<ul style="list-style-type: none"> Not used in the current study
Polyaniline (PANI)		<ul style="list-style-type: none"> Implantable electrodes, [10,19,25,54,26] Extensively used with mammalian cells Tissue engineering scaffolds [55–57] Bio-actuators [58–61] 	<ul style="list-style-type: none"> Not used in the current study
Poly(3,4-ethylenedioxy thiophene) doped with poly(styrene sulfonic acid) (PEDOT:PSS)		<ul style="list-style-type: none"> Extensively used with mammalian cells Substrate to regulate adhesion, proliferation and signaling of neuronal cells [7,62]; Electrical stimulation of embryonic P19 cells [20,42], neural stem cells [20,62] Coating of neural electrodes [36,40] 	<ul style="list-style-type: none"> Cytotoxicity tests Fibroblasts proliferation assay Electrical stimulation of NSCs during proliferation and differentiation
Poly(3-hexyl thiophene) (P3HT)		<ul style="list-style-type: none"> Used in Subretinal prosthetic implants [63] Photovoltaic devices, Light-emitting diodes (LEDs), transistors [64–67] Photo-stimulation of primary hippocampal neurons [68,69] 	<ul style="list-style-type: none"> Cytotoxicity assays;
Poly(9,9-dioctylfluorene- <i>alt</i> -bithiophene) (F8T2)		<ul style="list-style-type: none"> Not used with mammalian cells Transistors [70,71] Photovoltaic devices [72–74] Biosensors [75] 	<ul style="list-style-type: none"> Cytotoxicity assays; Fibroblasts proliferation assay
Poly(2-methoxy-5-(2'-ethyl)hexyloxy phenylene vinylene) (MEH-PPV)		<ul style="list-style-type: none"> Not used with mammalian cells LEDs [76]; Photovoltaic devices [76]; Biosensors [77] 	<ul style="list-style-type: none"> Cytotoxicity assays

stimulation, few reports exist on the effect of electrical stimulation applied through the conjugated polymer into mice embryonic stem cells, neural and muscle progenitor cells and a recent publication reports electrical stimulation of fetal human neural stem cells through PPy. PPy has also been applied to release drugs or growth factors [10,16–18], as well as to support growth of primary neurons, mesenchymal stem cells (MSCs) and NSCs when doped with immobilization factors such as extracellular matrix cell adhesion proteins or peptides [16,19–22]. The preparation and processing of PPy require techniques of cumbersome procedures such as in-situ interface polymerization that can impair wide applications. PPy can be also synthesized by chemical polymerization which offers some advantages including the large-scale low cost production and the flexibility to form PPy/synthetic polymer composites with desired properties for biomedical applications. The use of PPy alone as scaffold is limited due to its rigidity, insolubility, processability non-biodegradability and poor long term stability under electrical potential application [23,24]. Cui et al. studies revealed that PEDOT is electrochemically more stable than PPy, implying that PPy is not suitable for long term use in neural electrodes [25–28].

PANI has three distinct oxidation states with different colors [29] and its conductivity is strongly pH-dependent [30] At pH > 4 occurs the conversion from a conducting to a non-conducting form which strongly limits its application for monitoring biological processes [31–33]. PEDOT:PSS is a most promising candidate for long-term implantation in the central nervous system because, when compared to other conductive polymers such as PPy and PANI, it possesses several advantageous molecular properties: it combines a moderate bandgap located at the transition between the visible and near-IR regions of the spectrum (excellent optical transparency) [34], a low oxidation potential with good stability in the oxidized state [35] and has superior thermal and electrochemical stability [7]. Recently, PEDOT:PSS has been

employed in biomedical applications, such as coating of neural electrodes and nano-fiber electrodes due to its high charge delivery capacity leading to very low impedance and highly effective charge transfer, which results in higher signal-to-noise ratios for improved electrophysiological recordings [36–40]. It has also been used as substrate to regulate adhesion, proliferation and signaling of neuronal cells [39,41,42]. Recent studies showed that the PEDOT:PSS coated nanofibers are 3D scaffolds able to mimic the architecture of cell *niche* and able to regulate adhesion, proliferation and signaling of cells [43,44]. Cell electrospinning is a novel technique that allows the encapsulation of living cells within the fibers [45]. This approach will be tremendously useful for cell therapy, cell immobilization, for loading of therapeutic proteins that can then be subsequently released and for the development of disease models [46].

PEDOT:PSS is water soluble and over long term application in wet environments their films will tend to erode. Therefore, the cross-linker 3-glycidoxypropyltrimethoxysilane (GOPS) was added to the PEDOT:PSS aqueous dispersion. The films become cross-linked, upon hydrolysis and condensation of the silane groups which cause the formation of oligo/polysiloxane structures or networks that lock the PEDOT:PSS chains, thereby preventing its redispersion upon contact with water [78,79], improving the physical stability, while allowing the exploration of their superior molecular properties.

The current study aims to expand the application of conductive conjugated polymers on the electrical stimulation of human neural stem cells, together with cytotoxicity tests of two conjugated not previously assessed for biocompatibility, F8T2 and MEH-PPV. F8T2 is a photosensitive polymer with good hole-transporting properties and good stability against chemical doping by environment oxygen and water. It has been used in fabrication of organic photovoltaic cells [74,80]. MEH-PPV is a polymer that has low conductivity due to its low hole and electron mobilities and is currently used in electronic

applications (LEDs and photovoltaic cells). Nevertheless, this polymer offers an interesting property for biological application since it allows the immobilization of biomolecules due to its high density holes-traps [76,77].

Cross-linked PEDOT:PSS was also used in electrical stimulation, through application of a pulsed DC electric field to ReNcell VM progenitor cells. The ReNcell VM line is an immortalized human NSC (hNSCs) line derived from the ventral mesencephalon of ten-week gestation fetal neural tissue [81]. The ReNcell VM line retains a normal diploid karyotype even after long-term culture (>45 passages) and, when the growth factors EGF and FGF-2 are withdrawn from the medium, these cells undergo differentiation in neuronal and glial direction.

2. Materials and methods

2.1. Preparation of conducting polymer films

Different thin films were prepared by spin coating using conjugated polymer solutions. Namely:

- Cross-linked PEDOT:PSS: Ethylene glycol (Sigma-Aldrich) was added in a volume ratio of 1:4 to PEDOT:PSS (Heraeus, Clevios P AI 4083, solids content 1.3–1.7%) to increase the film electrical conductivity. Dodecylbenzenesulfonic acid (DBSA) (0.5 $\mu\text{L}/\text{mL}$) and 3-glycidioxypropyltrimethoxysilane (GOPS) (10 mg/mL) were added to the solution to improve film formation and stability, with GOPS acting as a cross-linking agent [82].
- P3HT, MEH-PPV: Poly (3-hexylthiophene) (P3HT) and poly-(2-methoxy-, -5-(2'-ethyl-hexyloxy)-*p*-phenylenevinylene) (MEH-PPV) were dissolved in chloroform.
- F8T2: poly(9,9-dioctylfluorene-*alt*-bithiophene) (F8T2) was dissolved in xylene.

Several coverslips were cleaned with isopropanol and dried with a nitrogen stream. The aqueous dispersions of cross-linkable PEDOT:PSS were spin coated on coverslips, (previously exposed to oxygen plasma (3 min) to enhance the hydrophilicity of their surface). The spin coating conditions were i) 1800 rpm (60 s) and post annealing (60°, 1 h) for the films used in cytotoxicity and fibroblast proliferation assays and ii) 1300 rpm (60 s) and post annealing (130°, 15 min) between each deposition (ten layers in total) for the experiments with electrical stimulation. The other polymers were spin coated on lamellas at 1500 rpm for 60 s suffering an annealing process of 150° for 2 min. The coverslips used in cell culture were sterilized with UV for 1 h 30 min in the case of cross-linked PEDOT:PSS substrate and with ethanol overnight for the other three substrates. Afterwards, they were stored in solutions of penicillin–streptomycin (1:100, Life Technologies) in phosphate buffer solution (PBS, Gibco) to maintain their sterility.

2.2. Conductivity measurement of PEDOT:PSS films

Cross-linked PEDOT:PSS films, deposited on glass, were coated with four 50 nm thick gold stripes (by thermal evaporation using an Edwards Coating System E 306A) in order to improve electrical contact during this physical characterization. Film resistance was measured using the four point probe method. The thickness of the films was measured using a Dektak 3.21 Profilometer.

2.3. Atomic force microscopy measurements

A Molecular Imaging (model 5100) Atomic Force Microscopy (AFM), operating in the noncontact mode, was used to obtain the topography of the substrates. Silicon cantilevers having a constant force in the range of 25–75 N/m and a resonant frequency ranging between 200 and 400 kHz were used. All images were taken with 512 \times 512 pixels resolution. The AFM images were processed using

second order plane fitting and second order flattening routines. The leveling routines were applied in order to remove the z offset between scan lines and the tilt and bow in each scan line. All AFM images were processed using the same leveling procedure with the final images indicating a flat planar profile, as expected. Gwyddion (version 2.9) software was used to process the AFM images. Current sensing AFM (CS-AFM), which makes use of a conductive tip, was used in the contact mode to simultaneously obtain topographical and current images of films deposited, by spin coating, on indium-tin oxide (ITO)-coated glass. Platinum–Iridium (PtIr) coated cantilevers (spring constant, 0.18–0.20 N/m) were used. The radius of the tip was 10 nm. The load force was maintained at 5–8 nN. A bias voltage between the ITO substrate and the conducting tip of 0.1 V was applied and the electrical current recorded during the films surface scanning. All AFM experiments were conducted under a nitrogen atmosphere to minimize moisture and adsorbed water effects. During current–voltage measurements at each position of the film, a bias voltage sweep (10 s) between -1 V and $+1$ V was applied.

2.4. Cytotoxicity assays and fibroblast adhesion and proliferation assays

Cytotoxicity assays: These were performed in vitro according to the ISO 10993-5:2009(E) guidelines in order to assess the biocompatibility of materials using the L929 mouse fibroblast cell line and Iscove's Modified Dulbecco's Medium (IMDM, Gibco) supplemented with 10% (v/v) of Fetal bovine serum (FBS, Gibco) as culture medium. For indirect contact assays, triplicates for each material were placed on 6-well plates (Falcon®, BD Biosciences) containing 2 mL of culture medium and kept in an incubator (37 °C, 5% CO₂, fully humidified) for 72 h. Then the liquid extracts were used to cultivate the L929 fibroblasts, seeded in 24-well plate (Falcon®, BD Biosciences) at an initial density of 8×10^4 cells/cm² for 48 h. Cell activity was quantified using the WST-1 kit (Roche) according to manufacturer instructions. Media incubated in tissue culture polystyrene or with a coverslip glass were used for the negative control and a piece of latex glove (toxic) as positive control. Direct contact assays were performed placing the test materials on the top of L929 fibroblasts cultures in 12-well plates near confluence and kept in an incubator (37 °C, 5% CO₂, fully humidified) for 24 h. After the incubation period, cells were observed under an inverted fluorescence microscope in order to qualitatively evaluate if they were confluent or if a halo of inhibition at cell material interface was formed.

Fibroblast adhesion and proliferation assays: the coverslips with spun coated cross-linked PEDOT:PSS and F8T2 were glued using a biocompatible glue FDA approved (Silastic® medical adhesive silicone, type A) on 24-wells ultra-low attachment plate. This operation was carried out in the laminar chamber and wells were washed with a solution of pen-strep (1:100) in PBS to ensure material sterility. A glass cover slip without coated substrate was used as positive control. The coverslips with polymers were incubated (37 °C, 5% CO₂, in a fully humidified environment) with IMDM containing 10% (v/v) FBS for 1 h. After that, cells were plated at 15,000 cells/cm² in IMDM + 10% FBS. The cells were counted in a hemocytometer using the Trypan Blue (Gibco, Invitrogen) exclusion test.

2.5. ReNcell VM culture

ReNcell VM (Millipore®) is an immortalized human neural progenitor cell line that was derived from the ventral mesencephalon region of a human fetal brain tissue and that was immortalized by retroviral transduction with the v-myc oncogene. This cell line has the ability to differentiate into neurons and glial cells [81]. ReNcell VM cells were expanded and harvested as described elsewhere [83]. Cells were then plated at an initial cell density of 140,000 cells/cm² in DMEM medium supplemented with EGF

(20 ng/mL, Peprotech), FGF-2 (20 ng/mL, Peprotech) and B27 (20 ng/mL, Life Technologies) on cross-linked PEDOT:PSS coated with poly-L-Ornithine (Sigma, 15 µg/mL, 30 min, at 37 °C) and laminin (Sigma, 20 µg/mL, 3 h at 37 °C), at 37 °C and 5% CO₂ humidified environment. The medium was renewed every 2 days during proliferation. After 4 days in culture, EGF and FGF-2 were withdrawn from the culture medium, and NSCs underwent differentiation into neuronal and glial lineages. The differentiation process was carried out for 8 days, using a 1:1 mixture of DMEM/F12 supplemented with N2 with Neurobasal medium (Life Technologies) supplemented with B27 (1×), and changing the medium every 3 days.

To avoid cell dispersion, a ring of a biocompatible glue FDA approved (Silastic® medical adhesive silicone, type A) was made on the top of the cross-linked PEDOT:PSS substrate. Two parallel strips of gold with 40 nm of thickness were deposited outside the edges of the ring. Platinum wires (Sigma-Aldrich®) were connected to these strips and an external power supply, connected to the electrodes, was used to apply a pulsed DC electric field vector that runs horizontally along the substrate perpendicular to the gold strips (scheme shown in Fig. 1A). The cells were exposed to pulsed stimulation potential, with a frequency of 100 Hz for 24 h during the first 4 days and over 12 h during differentiation time (following 8 days), according to the culture time

schedule shown in Fig. 1B. The distance between the electrodes was 1 cm, so the generated electric field was 1 V/cm.

2.6. ReNcell VM characterization

2.6.1. NSCs elongation

The elongation of adherent NSCs on conductive PEDOT:PSS was investigated after 4 days of culture using SEM imaging. The cells were fixed with glutaraldehyde 1,5% (v/v) in PBS at 37 °C for 1 h. The samples were washed three times with PBS and afterwards the samples were immersed in ethanol solutions at different concentrations, 25%, 50%, 75% and 99% for 30 min each at 37 °C. Before the observation of the substrates they were coated with a 30 nm Au/Pd layer using a Polaron model E5100 coater (Quorum Technologies). Images were obtained using a Field Emission Gun Scanning Electron Microscope (FEG-SEM) (JEOL, JSM-7001F model). Elongation of cells was assessed by measuring the aspect ratio (ratio between the short axis divided by the long axis), as shown in Eq. (1). An aspect ratio of 1 corresponds to a circular like cell and an aspect ratio of 0 corresponds to an infinitely stretched cell. More than 30 cells were characterized.

$$\text{Aspect ratio (AR)} = \text{length of minor axis} / \text{length of major axis. (1)}$$

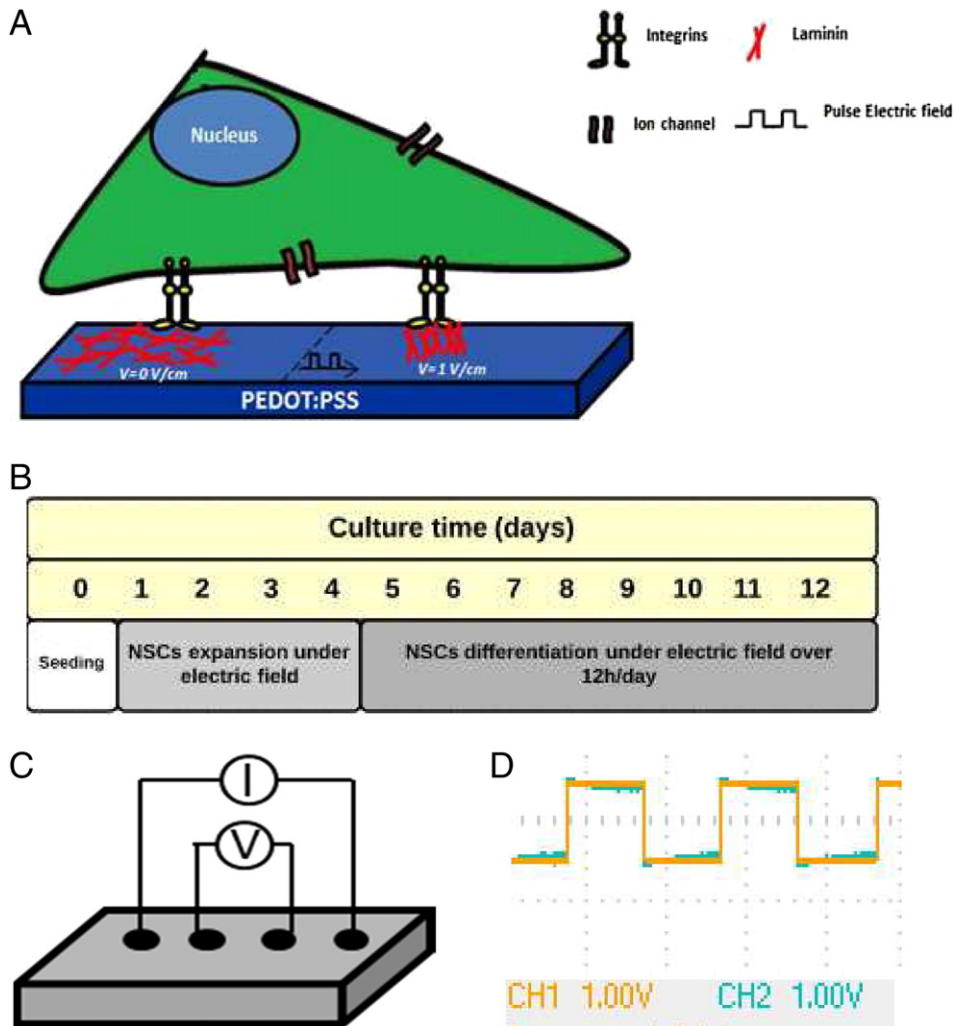


Fig. 1. A) In this work it was hypothesized that the application of a proper electric field through cross-linked PEDOT:PSS substrate induces a steer of laminin towards the surface improving their binding to cell integrins resulting in an different behavior of NSCs comparatively to control (without electric field). B) Experimental scheme with the electrical stimulation during the NSC proliferation and differentiation. C) The four-point probe setup. A high impedance current source supplies a current through the outer two probes and a voltmeter measures the voltage across the inner two probes in order to determine sample resistivity. D) An example of the pulsed voltage waveform (CH1) used, superimposed with the output voltage obtained (CH2).

2.6.2. NSCs differentiation

Differentiation of NSCs at the end of the culture period was evaluated through cells immunostaining for the neuronal marker β -III Tubulin (Tuj1) and for astrocyte marker glial fibrillary acidic protein (GFAP). Cells were fixed with PFA 4% (2 mL per well of six well-plate) for 30 min at room temperature, and then washed twice with PBS. Cells were incubated for 30 min at room temperature with blocking solution (PBS with 0,1% Triton X-100 and 10% NGS) and, after this, the primary antibodies diluted (Tuj1 1:2000, GFAP 1:100) in staining solution (PBS with 0,1% Triton X-100 and 5% NGS) were incubated at 4 °C overnight. After the incubation with the primary antibody, cells were washed once with PBS and incubated with the appropriate secondary antibody (Life Technologies, dilution 1:500) for 1 h at room temperature in a dark container. Finally, cells were washed once with PBS, incubated with DAPI for 2 min at room temperature and washed twice with PBS. The stained cells were visualized under a fluorescence microscope (Leica DMI 3000B).

2.6.3. Neurite length quantification

The plug-in NeuronJ is a semi-quantitative method that allows the measurement of neurites in neurons. First, the background fluorescence is subtracted with a rolling ball radius of 50 pixels. Then a color threshold is defined in order to enhance the contrast between neurites and other particles. The image is then binarized, rendering positively stained particles the maximum intensity (shown in dark) against zero intensity particles (in white). Through the NeuronJ plug-in, tracings are created by placing the cursor at one end of the cell, stretching the tracing, which is automatically calculated by the software, until the other end of the cell. The tracings are then automatically measured.

3. Results and discussion

3.1. Conjugated polymer-based surface characterization

Two conjugated polymers that were previously used to interface cells (P3HT and PEDOT:PSS) are studied in the present work and another two (F8T2 and MEH-PPV) were for the first time assessed as non-cytotoxic. PEDOT:PSS, which has a high conductivity and transparency in the visible range, has been extensively studied concerning cell-materials interface. However, this material is water soluble impairing long term applications, therefore in the current study PEDOT:PSS was cross-linked with GOPS. Additional characterization of cross-linked PEDOT:PSS surfaces, alone or coated with laminin, an adhesion protein of the extracellular matrix, is carried out.

3.1.1. Cytotoxicity, cellular viability, cell adhesion and proliferation

Indirect and direct cytotoxic tests were performed for each conjugated polymer following the ISO 10993-5 guidelines for medical devices. The materials were incubated with IMDM supplemented with 10% (v/v) FBS for 72 h and the resulting liquid extracts were used as media for indirect tests using L929 fibroblasts cells. The values of cell metabolic activity obtained using the reagent WST-1 (Fig. 2A), normalized against tissue culture polystyrene (negative control), and the morphology of the cells (data not shown) showed that none of the polymer lixiviates has cytotoxic effects. Also in assays for direct contact between cells and polymers (data not shown), no inhibition halo was observed. Therefore, according to the ISO used these polymers are non-cytotoxic.

Additional studies with L929 fibroblast cells targeted the ability of mammalian cells to adhere and proliferate on two of the conjugates polymers (CP) without application of electrical field or the use of protein coatings, exploring the ability of conjugated polymer surface charge to stimulate cell adhesion. Considering the higher PEDOT:PSS conductivity and enhanced stability provided by the cross-linking procedure and the interesting photophysical properties of F8T2, these

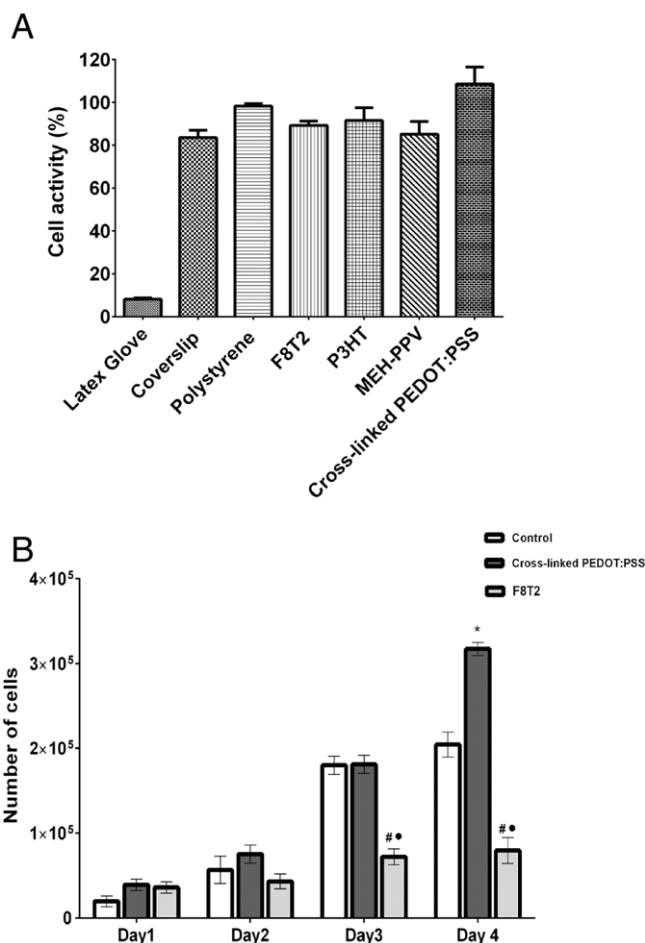


Fig. 2. A) Cytotoxicity assays for P3HT, F8T2, MEH-PPV, and cross-linked PEDOT:PSS, following the ISO standards for biomaterials with tissue culture plate (polystyrene) as negative control and a piece of latex glove (toxic) as positive control. B) Fibroblast growth in polymers without coating. Glass coverslip was used as positive control. Bars represent mean \pm SEM of at least 3 replicates. Statistical analysis was performed by repeated measures two-way ANOVA followed by Tukey's Multiple Comparison Test (# and * denotes $p < 0.0001$ comparing F8T2 and PEDOT to control, * denotes $p < 0.0001$ comparing F8T2 to cross-linked PEDOT).

two CP were tested for adhesion and proliferation over 4 days. A glass coverslip was used as positive control. The morphology (shape and appearance) of cells inspected by a microscope at day 2 (data not shown), confirms the healthy status of cells without any signs of contamination or detachment of the cells from the substrates. The results obtained (Fig. 2B) show that, after 24 h of culture, the relative number of cells on the cross-linked PEDOT:PSS surface is similar to the number of cells on F8T2 and larger than the number of cells on the control plate. After 4 days in culture, the cells on the surfaces coated with cross-linked PEDOT:PSS increase 9-folds with respect to the initial value, which represents a proliferation that is 1.3 times higher than for the glass coverslip control; while a lower proliferation was observed for spin coated F8T2 with a 2.4-cell-fold increase over the same period. The cell viability assessed by trypan blue exclusion method [84] was superior to 90% for all the substrates, therefore these conducting polymers present an excellent behavior as substrate to support cellular adhesion and proliferation suggesting its potential role as scaffold for tissue engineering. These results clearly show that cross-linked PEDOT:PSS is not cytotoxic and provides superior properties to promote mammalian cell adhesion and proliferation.

3.1.2. Electrical characterization of cross-linked PEDOT:PSS

The conductivity of cross-linked PEDOT:PSS was obtained using the four-point probe techniques. The four-point probe method relies on the

application of a constant current across two outer electrodes at the surface of the material and on the measurement of the potential difference between the inner pair of electrodes. The resistivity of PEDOT:PSS thin films was calculated using Eq. (2):

$$\rho = RLw/l \quad (2)$$

where ρ is the resistivity, R is the resistance, L is sample width, w is the sample thickness and l the distance between the two inner contacts. The conductivity ($\sigma = 1/\rho$) obtained for cross-linked PEDOT:PSS films was $5.8 \Omega^{-1} \text{ m}^{-1}$.

3.1.3. Atomic force microscopy studies

Adult stem cells reside in particular cellular microenvironment or niche that provides cues essential to the maintenance of stem cell population [85,86]. Such niche is comprised by cells, solute factors and extracellular matrix (ECM) molecules which include adhesion molecules, such as the laminin [87]. Neural stem cell culture is usually quite stringent when considering adhesion factors, with laminin being the adhesion protein recommended to support the model neural stem cell selected for this study, ReNCell VM cell line [83]. Therefore, in this work, cross-linked PEDOT:PSS surfaces were coated with laminin by drop casting, to maintain and improve growth, proliferation and differentiation of NSCs. Before proceeding for the AFM studies, the substrates were washed with distilled water to remove unbound laminin. Substrates of cross-linked PEDOT:PSS were also characterized after immersion in distilled water.

Surface topology has a high impact on cell adhesion and proliferation with surfaces with higher roughness improving cell culture performance [88–91]. Therefore, noncontact AFM studies of the cross-linked PEDOT:PSS, cross-linked PEDOT:PSS after being immersed in distilled H_2O and cross-linked PEDOT:PSS coated with laminin were performed to characterize surface morphology. As mentioned above, the AFM study of the cross-linked PEDOT:PSS substrates coated with laminin was performed after their cleansing with distilled water to remove the excess of laminin that didn't adhere to PEDOT:PSS surface.

Fig. 3 shows the obtained topographic and phase images ($0.5 \times 0.5 \mu\text{m}^2$). The phase image has white and dark regions, which, by forming a pattern different from the topography contrast, indicate that domains of different chemical components exist at the surface. In other words, the phase image shows that phase separation occurs at the PEDOT:PSS surface. This is in line with previous AFM studies [92]. Ionescu-Zanetti et al., identified the softer material as PEDOT and the harder material as PSS [93,92]. The two polymer domain separation is more evident in the phase image of cross-linked PEDOT:PSS than in the phase image of cross-linked PEDOT:PSS immersed in distilled H_2O .

Adsorption of laminin, the ECM molecule used in this studied, on cross-linked PEDOT:PSS surface was also studied using non-contact AFM, since laminin is an essential factor to promote NSCs adhesion. Differences between phase images from cross-linked PEDOT:PSS alone and surfaces coated with laminin are found. Nevertheless, topographic images obtained with noncontact AFM do not allow distinguishing laminin from the PEDOT:PSS substrate, either as prepared or after being immersed in distilled water

The root-mean-square roughness (R_{rms}) was calculated for $1 \times 1 \mu\text{m}^2$ topographic images and the results are summarized in Table 2. There is an evidence that laminin adsorbs on PEDOT:PSS surface, the R_{rms} increase from 2.6 ± 0.30 to 7.0 ± 0.01 nm upon coating of the PEDOT:PSS surface with laminin is consistent with its adsorption.

In order to confirm the indications of laminin adsorption provided by the increase in the surface roughness, in particular with respect to the PEDOT:PSS substrate that was immersed in water, further studies using Current-Sensing AFM (CS-AFM) technique were carried out in a contact mode. This technique provides simultaneous information of the surface topography and on the current distribution across the sample. However, we could not obtain good topographic images for the cross-linked PEDOT:PSS coated with laminin (data not shown), since the tip dragged along the laminin adsorbed at cross-linked PEDOT:PSS surface. Nevertheless, from the electrical current mapping images of cross-linked PEDOT:PSS alone and coated with laminin, we can estimate that the regions with high conductivity correspond to 50% and 2% of the $1 \times 1 \mu\text{m}^2$ scanned area, respectively. This implies that laminin coating was effective for a large surface area. Fig. 4 shows that the laminin covers the cross-linked PEDOT:PSS surface promoting a decrease of the number of the high current domains. Compared to the surface coated with laminin, the histogram obtained for the substrate made of cross-linked PEDOT:PSS alone has higher current values, where a significant number of regions with currents between 1 and 10 nA were detected. The electrical current histogram of laminin presents lower current values, but indicates a significant number of regions with currents between 0.1 and 1 nA, allowing assessing the effect of current stimulation on neural stem cells fate.

3.2. Effect of electrical stimulation in neural stem cell fate

In this study, cross-linked PEDOT coated with laminin is engineered as a biocompatible conductive substrate for application of pulsed DC electric field, allowing studying the effect of pulsed electrical current on NSCs expansion and differentiation processes. The electrical field was applied by parallel electrodes spaced by one centimeter and the direction of electrical field was parallel to the sample surface. Application of electrical fields of 1–2 V/cm occurs during morphogenesis and wound healing and has been shown to orient the movements of a wide variety

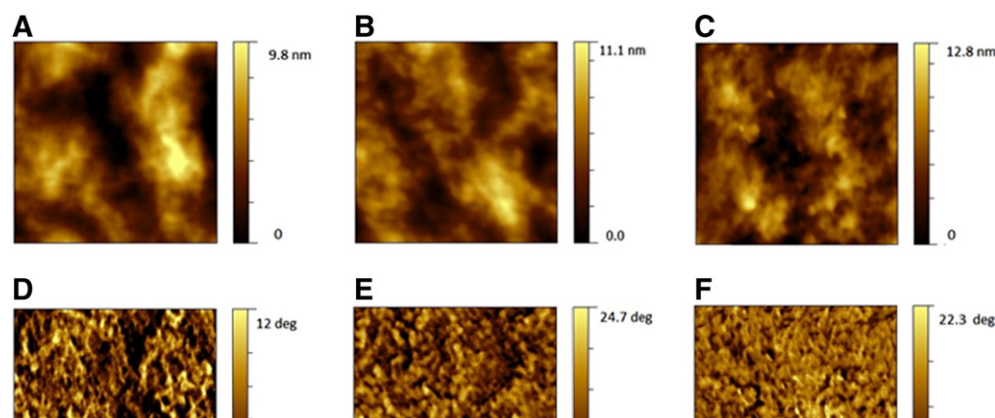


Fig. 3. Topography (A,B,C) and phase(D,E,F) AFM images of (A,D) cross-linked PEDOT:PSS, (B,E) cross-linked PEDOT:PSS immersed in distilled water and (C,F) cross-linked PEDOT:PSS coated with laminin. The images were obtained with noncontact mode over an area of $0.5 \times 0.5 \mu\text{m}^2$.

Table 2
Root-mean-square roughness (R_{rms}) of the different surfaces.

Surface	R_{rms} (nm)
PEDOT:PSS	2.60 ± 0.30
PEDOT:PSS immersed in distilled H ₂ O	2.20 ± 0.01
Laminin/PEDOT:PSS	7.00 ± 0.01

of cells in vitro [94]. Taking this into account and also in order to avoid the electrolysis of water (that occurs at 1.2 V) that would change pH of medium, 1 V was the magnitude chosen to be applied.

3.2.1. Elongation of neural stem cell under electrical stimulus

Cell elongation is one of the adaptation methods that cells undergo in order to perform certain functions and through which they connect to adaptor proteins and push their membrane in the direction of movement [95,96]. Modulation of cell morphology and cytoskeletal organization play an important role in stem cell lineage commitment [96,97]. In the current study, neural stem cells were first cultivated for 4 days in the presence of factors (EGF, FGF-2) and B27 supplement that promote maintenance of NSC multipotency.

Considering that neural stem cell stretching can lead their differentiation towards higher number of longer neurons [98–102], elongation of the NSC after 4 days in culture was quantified through cell aspect ratio measurements. Aspect ratios (AR) were measured analyzing SEM images using ImageJ software for cell populations of at least 30 cells cultivated in cross-linked PEDOT:PSS coated with laminin, either under the presence or absence of pulsed electrical current.

The results, presented in Fig. 5, show statistically significant different aspect ratios for the cell populations that were or were not electrically stimulated, of 0.24 ± 0.09 and 0.54 ± 0.09 , respectively. In response to the external pulsed DC electrical field, cells elongate and stretch significantly when compared with the cell populations not submitted to electrical stimulation. Several reports showed that electrical stimulation affects actin cytoskeleton reorganization which may be responsible

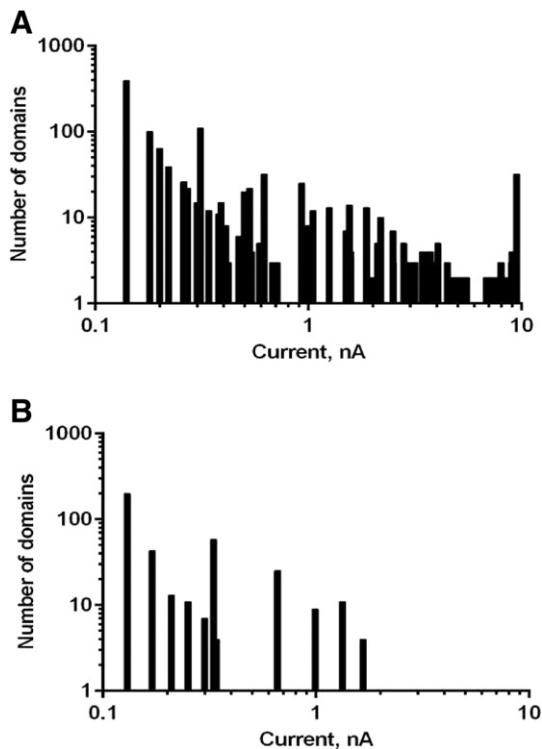


Fig. 4. Electrical current histogram of cross-linked PEDOT:PSS alone (A) and coated with adsorbed laminin (laminin/PEDOT:PSS) for $1 \times 1 \mu\text{m}^2$ scanned area.

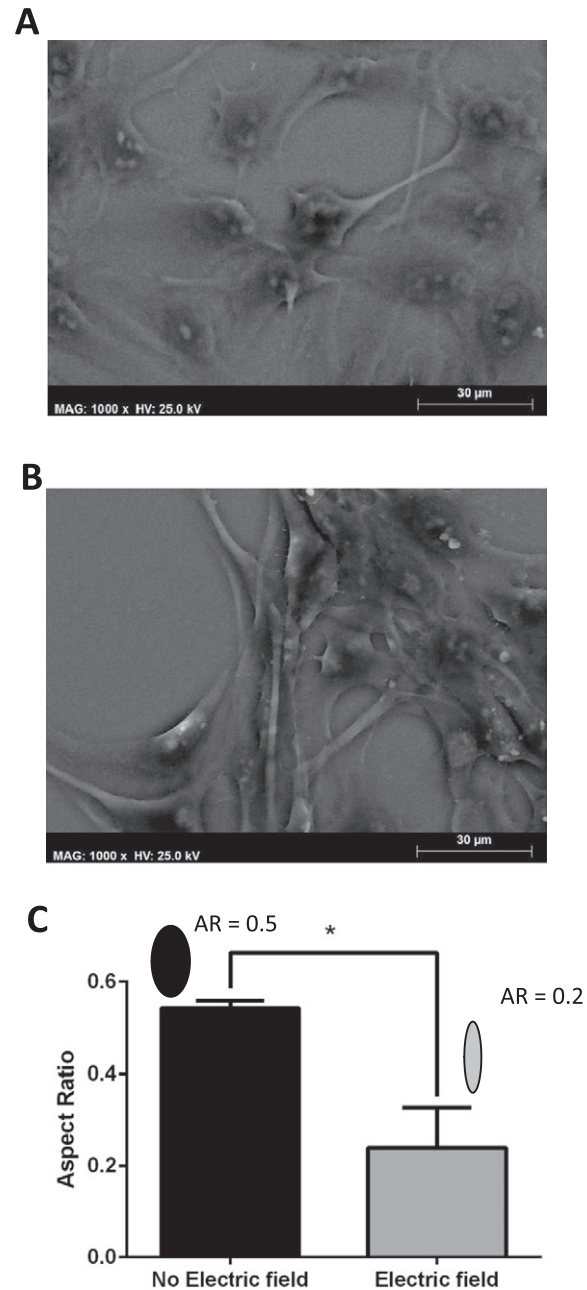


Fig. 5. SEM images of NSCs on cross-linked PEDOT:PSS substrates without (A) and with (B) electric field stimulation. Cell elongation quantification by aspect ratio ($AR = \text{minor axis}/\text{major axis}$), where $AR = 1$ corresponds to a perfect circle and $AR = 0$ to a fully elongated shape. More than 30 cells were analyzed. * Values are statistically significant different ($p < 0.05$). Ellipses with AR similar to the average values obtained are represented in the figure for illustration purposes.

for the cell morphological changes here described, particularly the cell stretching [42,94,103,104]. Ellipses with AR similar to the average values obtained are represented in the figure for illustration purposes.

Several studies showed that the electrical stimulation across the substrate promotes a redistribution of the cell surface receptors [105,106] and alters the recruitment and the adsorption of proteins [1,16,107]. The large amount of protein (such as laminin) adsorbed on polymer surface and the up-regulation of growth factor receptors induced by electrical stimulation, may promote a cytoskeletal reorganization resulting in cell morphological changes. Our results are in agreement with other published studies [100,108] and suggest that the electric field strength with AC frequency was strong enough to affect cell morphology. To our knowledge, the precise mechanisms by which

cells respond to AC electric signals are still not known, so further investigation is required to address this question.

Many of the human cells respond to endogenous in-vivo electrical stimulation, but neuronal cells are specifically designed to transmit electrical impulses along the human body, allowing receiving and processing information. In vivo, in wound healing, electrical currents of 4–10 $\mu\text{A}/\text{cm}^2$ are observed [109,110]. Therefore, one can hypothesize that an ideal neural scaffold should possess electrical conductivity to promote neurite outgrowth and enhance nerve regeneration in culture, developing better disease models, drug screening systems, neuroprosthetic devices or neural probes. The physiological function of in vitro cultured cells could be altered in response to physical stimuli as electric stimulation, mechanical force and topography [111–114]. Electrical stimulation can be a source of directional cues in vitro to control cellular processes including microfilament reorganization, elongation, gene expression, differentiation and migration of NSCs towards specific targets [115–118]. However, the response to electric stimulation is diverse depending on cell type, developmental stage, and species [119,120].

3.2.2. Electrical stimulation effect on NSC differentiation

Adult neural stem cells residing in their natural niche, when recruited for tissue repair or regeneration can differentiate in neurons or glial cells, the later ones providing nutrition and operational support for the neurons. In the current study, after an NSC expansion period of 4 days, an additional period of 8 days of non-specific differentiation was carried out, changing the medium every 3 days. No other factors directing specifically for neuron or glial cell lineage were added. The NSCs expanded under electrical stimulation were also differentiated under electro stimulation, but instead of applying pulsed current 24 h a day, the cells were submitted to electrical stimulation during 12 h a day. The second

set of cells was also expanded on cross-linked PEDOT:PSS coated with laminin, but in the absence of electrical stimulation. They, were also submitted by differentiation stage (using media without multipotency factors) in the absence of electrical stimulation.

Immunofluorescence study was performed using specific antibodies against Tuj1, which labels neurons in early development stage as well as mature neurons and GFAP to identify the differentiated level of astrocytic populations. The NSCs on cross-linked PEDOT:PSS substrates under and without electrical stimulation, differentiated into neurons and into astrocytes confirmed by Tuj1 and GFAP immunoreactivity, respectively (Fig. 6). ImageJ software quantification indicates that the electrical stimulation increases the percentage of Tuj1-positive cells, being this statistically significant (Fig. 6D).

Previous studies also suggest that conductivity of substrate can be an essential factor for differentiation and determination of cell fate [20]. The electrical stimulation influences the neuronal differentiation, so, when the conductive electrically cross-linked PEDOT:PSS substrate was placed into an electrolyte solution, it was able to sustain local electrochemical currents between the substrate and cell monolayer. Yanes et al., manipulated several-signaling pathways in embryonic stem cells to understand how the stem cell redox state is regulated during differentiation [121]. Their results are in agreement with other previous studies that revealed that the balance between self-renewal and differentiation state is regulated by intracellular oxidation state [122,123]. We suggest that redox reactions between the conductive surface and cell monolayer may have changed the intracellular distribution of redox couples and, consequently, the intracellular redox potential, regulating in this way cell differentiation. Changes in the effective redox potential may alter the conformation of proteins [124] or may stimulate signaling molecules that make cells more oxidized, which is has been suggested as a prerequisite for neural differentiation.

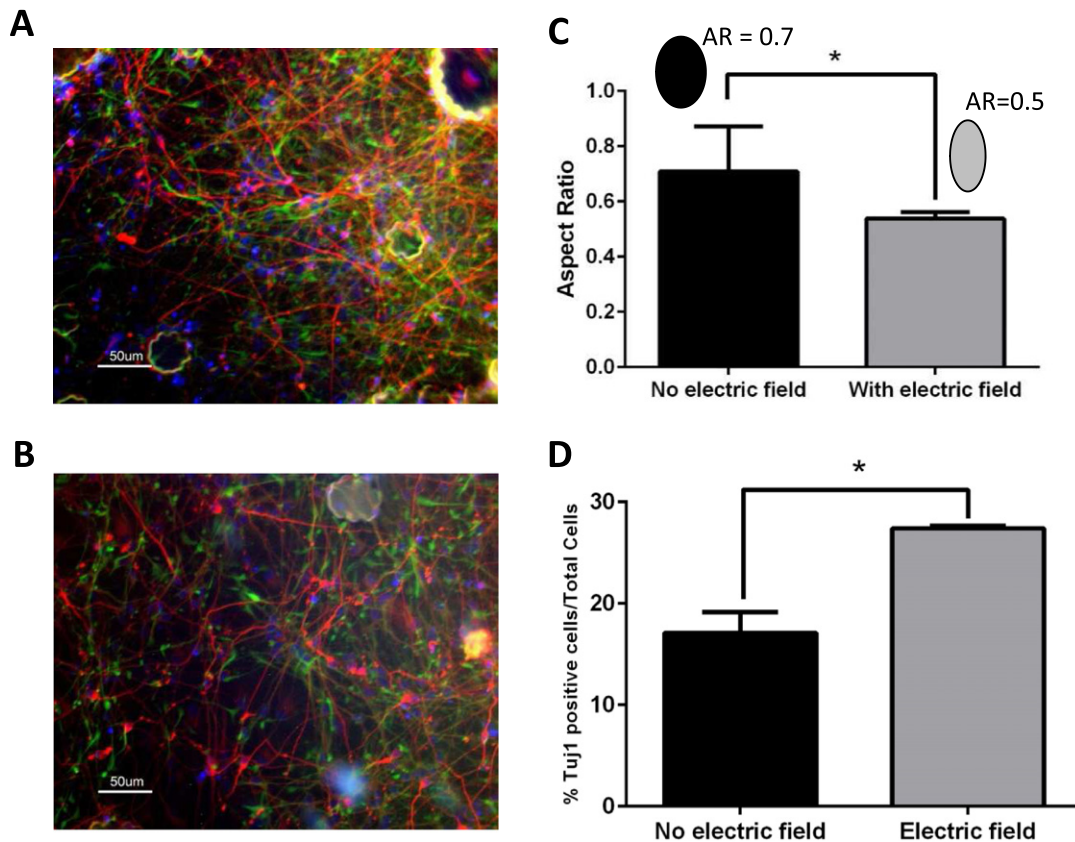


Fig. 6. Immunofluorescence images of anti-Tuj1 (red) and anti-GFAP (green) followed by DAPI (blue) staining for the nuclei of the fetal NSCs on cross-linked PEDOT:PSS. NSCs differentiation occurred on cross-linked PEDOT:PSS substrates without (A) and with (B) electric stimulation. (C) Quantification of aspect ratio of neurons. More than 30 cells were analyzed. (D) Quantification of percentage Tuj1 positive. * Represents statistically significant differences between average values obtained ($p < 0.05$), using cell populations higher than 20.

There may be a link between cell elongation or electrical stimulation over the expansion and differentiation towards neuron lineage, since the differentiation of NSC towards this lineage was higher when starting from NSC with higher aspect ratios (Fig. 6). The aspect ratio of neurons obtained in cultures submitted to electrical stimulation is also statistically significant lower, corresponding to longer neurons, confirming a positive effect on NSC differentiation towards these cells types.

3.2.3. Electrical stimulation enhances neurite outgrowth

The neurite outgrowth is a complex and fundamental process during neuronal migration and differentiation. This process begins with the neurite formation, being followed by elongation of neurites over long distances and guidance through tissues in order to recognize proper targets where the synapse formation and functional maturation of the newly formed connections occurs.

Several reports argue that the application of external electric fields (EF) promotes galvanotaxis of cell, directing cell movement towards the anode or the cathode [115,125–127]. An assessment of the pulsed DC electric field on the neurite length measured from differentiated fetal NSCs was performed. (Fig. 7). The average neurite length was $73 \pm 5 \mu\text{m}$ under control culture condition (no electric field applied), but a statistically significant longer neurite, with an average value length of $108 \mu\text{m} \pm 7$ was measured at the field strength of 1 V/cm. The results inhere obtained agree with other reports in the literature that show that the application of an electrical stimulus increases the neurite outgrowth [47,49,128–130].

The mechanisms by which electrical stimulation regulates neurite outgrowth are unknown but several theories have emerged to explain it. Namely, the electrical stimulation (a) can regulate intracellular signaling pathways and also interact with cytoskeletal proteins that modulate the morphology and migration of the growth cone [131], (b) can increase protein synthesis and (c) favor the ECM protein conformational changes [47]. In this study, electrical charges pass through the cross-linked PEDOT:PSS film on which cells are attached via laminin monolayer. It is likely that the passage of electronic current through the material, and not the ionic flow of current through the electrolyte medium, is responsible for the enhancement of neurite extension. Other plausible explanations are that the electrical stimulation upregulated the protein synthesis in neurons or increased the adsorption of nutrients and proteins from the medium [16].

4. Conclusions

This study confirms that two materials previously studied for conjugated polymer-cell interface (P3HT and PEDOT:PSS) are not cytotoxic and demonstrates for the first time that two other conjugated

polymers (F8T2 and MEH-PPV) are also non-cytotoxic. PEDOT:PSS presents a high conductivity and transparency, and has been extensively studied concerning cell-materials interface. However, this material is water soluble impairing long term applications, therefore in the current study PEDOT:PSS was first cross-linked with GOPS. This stable cross-linked PEDOT:PSS facilitates material manufacture for use in biological systems, without the need of in-situ polymerization of the conjugated polymer usually performed to gain stability. Cell adhesion and proliferation were assessed using L929 fibroblasts with cultures in the cross-linked PEDOT:PSS being higher than in pre-optimized commercial tissue culture flasks, while F8T2 presents moderate proliferation. Laminin coating increases the roughness of the cross-linked PEDOT:PSS and reduces the exposed conductive domains (PEDOT-based), indicating that laminin does bind to the PEDOT:PSS surface. At the end of the expansion stage, ReNcell VM neural stem cells were more elongated for the electrically stimulated populations. The population of neurons (labeled as Tuj1) obtained under electrical stimulus was higher than in its absence. Notice that the differentiation that was carried out was not specifically designed towards neuron differentiation. Again neurons obtained under electrical stimulus present higher elongations and longer neurites, compared to those obtained in its absence. Summing up, this work demonstrates that the use of electro-conductive conjugated polymers, in particular cross-linked PEDOT:PSS, can successfully be used, through the application of a pulsed current, to elongate neural stem cells impacting on their differentiation in higher percentages of neurons and contributing to a higher elongations and longer neurites, when cultivated under an electrical current.

Transparency Document

The <http://dx.doi.org/10.1016/j.bbagen.2015.01.020> Transparency Document associated with this article can be found, in the online version.

Acknowledgments

We thank Fundação para a Ciência e Tecnologia (FCT) through the following initiatives: MIT-Portugal Program - Bioengineering Systems Focus Area, Projects UID/EEA/50008/2013, postdoc grant (SFRH/BPD/75338/2010) to QF and SFRH/BPD/82056/2011 to CAVR and contract IF/00442/2012 to FCF.

Appendix A. Supplementary data

Supplementary data to this article can be found online at <http://dx.doi.org/10.1016/j.bbagen.2015.01.020>.

References

- [1] J.Y. Wong, R. Langer, D.E. Ingber, Electrically conducting polymers can noninvasively control the shape and growth of mammalian cells, *Proc. Natl. Acad. Sci.* 91 (1994) 3201–3204.
- [2] R. Ravichandran, S. Sundarajan, J.R. Venugopal, S. Mukherjee, S. Ramakrishna, Applications of conducting polymers and their issues in biomedical engineering, *J. R. Soc. Interface* 7 (2010) S559–S579.
- [3] N.K. Guimard, N. Gomez, C.E. Schmidt, Conducting polymers in biomedical engineering, *Prog. Polym. Sci.* 32 (2007) 876–921.
- [4] K. Aboody, A. Capela, N. Niazi, J.H. Stern, S. Temple, Translating stem cell studies to the clinic for CNS repair: current state of the art and the need for a Rosetta Stone, *Neuron* 70 (2011) 597–613.
- [5] T. Gorba, L. Conti, Neural stem cells as tools for drug discovery: novel platforms and approaches, *Expert Opin. Drug Discov.* 8 (2013) 1083–1094.
- [6] Z. Kokaia, G. Martino, M. Schwartz, O. Lindvall, Cross-talk between neural stem cells and immune cells: the key to better brain repair [quest], *Nat. Neurosci.* 15 (2012) 1078–1087.
- [7] J.E. Collazos-Castro, J.L. Polo, G.R. Hernández-Labrado, V. Padiá-Cañete, C. García-Rama, Bioelectrochemical control of neural cell development on conducting polymers, *Biomaterials* 31 (2010) 9244–9255.
- [8] A. Subramanian, U.M. Krishnan, S. Sethuraman, Development of biomaterial scaffold for nerve tissue engineering: biomaterial mediated neural regeneration, *J. Biomed. Sci.* 16 (2009) 108.

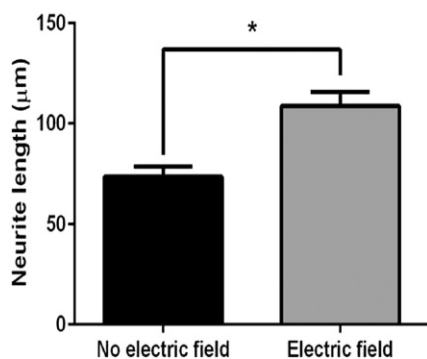


Fig. 7. Differentiated ReN cells cultured in cross-linked PEDOT:PSS substrates with and without electric stimulation were immunostained against neuronal-marker Tuj1. Fluorescence microscopy images were analyzed and mean length of neurites was measured in each condition. Results are displayed as the mean of 26 measurements ($n = 26$) in an image of each condition. * indicates statistically significant difference between values ($p < 0.05$).

- [9] X. Wang, et al., Evaluation of biocompatibility of polypyrrole in vitro and in vivo, *J. Biomed. Mater. Res. A* 68 (2004) 411–422.
- [10] P.M. George, et al., Fabrication and biocompatibility of polypyrrole implants suitable for neural prosthetics, *Biomaterials* 26 (2005) 3511–3519.
- [11] S. Bhadra, D. Khatgir, N.K. Singha, J.H. Lee, Progress in preparation, processing and applications of polyaniline, *Prog. Polym. Sci.* 34 (2009) 783–810.
- [12] W.-S. Huang, B.D. Humphrey, A.G. MacDiarmid, Polyaniline, a novel conducting polymer. Morphology and chemistry of its oxidation and reduction in aqueous electrolytes, *J. Chem. Soc. Faraday Trans.1: Phys. Chem. Condens. Phases* 82 (1986) 2385–2400.
- [13] M. Mattioli-Belmonte, et al., Tailoring biomaterial compatibility: in vivo tissue response versus in vitro cell behavior, *Int. J. Artif. Organs* 26 (2003) 1077–1085.
- [14] M. Asplund, et al., Toxicity evaluation of PEDOT/biomolecular composites intended for neural communication electrodes, *Biomed. Mater.* 4 (2009) 045009.
- [15] D. Kumar, R. Sharma, Advances in conductive polymers, *Eur. Polym. J.* 34 (1998) 1053–1060.
- [16] A. Kotwal, C.E. Schmidt, Electrical stimulation alters protein adsorption and nerve cell interactions with electrically conducting biomaterials, *Biomaterials* 22 (2001) 1055–1064.
- [17] V. Lundin, A. Herland, M. Berggren, E.W. Jager, A.I. Teixeira, Control of neural stem cell survival by electroactive polymer substrates, *PLoS One* 6 (2011) e18624.
- [18] Y. Li, K.G. Neoh, E.-T. Kang, Plasma protein adsorption and thrombus formation on surface functionalized polypyrrole with and without electrical stimulation, *J. Colloid Interface Sci.* 275 (2004) 488–495.
- [19] X. Cui, J. Wiler, M. Dzaman, R.A. Altschuler, D.C. Martin, In vivo studies of polypyrrole/peptide coated neural probes, *Biomaterials* 24 (2003) 777–787.
- [20] E. Ostrakhovitch, J. Byers, K. O'Neil, O. Semenikhin, Directed differentiation of embryonic P19 cells and neural stem cells into neural lineage on conducting PEDOT-PEG and ITO glass substrates, *Arch. Biochem. Biophys.* 528 (2012) 21–31.
- [21] H. Castano, E.A. O'Rear, P.S. McFetridge, V.I. Sikavitsas, Polypyrrole thin films formed by admicellar polymerization support the osteogenic differentiation of mesenchymal stem cells, *Macromol. Biosci.* 4 (2004) 785–794.
- [22] L. Zhang, W.R. Stauffer, E.P. Jane, P.J. Sammak, X.T. Cui, Enhanced differentiation of embryonic and neural stem cells to neuronal fates on laminin peptides doped polypyrrole, *Macromol. Biosci.* 10 (2010) 1456–1464.
- [23] G. Shi, M. Rouabhia, Z. Wang, L.H. Dao, Z. Zhang, A novel electrically conductive and biodegradable composite made of polypyrrole nanoparticles and polylactide, *Biomaterials* 25 (2004) 2477–2488.
- [24] C. Thomas, K. Zong, P. Schottland, J. Reynolds, Poly (3, 4-alkylenedioxythiophene)s as highly stable aqueous-compatible conducting polymers with biomedical implications, *Adv. Mater.* 12 (2000) 222–225.
- [25] X. Cui, J.F. Hetke, J.A. Wiler, D.J. Anderson, D.C. Martin, Electrochemical deposition and characterization of conducting polymer polypyrrole/PSS on multichannel neural probes, *Sensors Actuators A Phys.* 93 (2001) 8–18.
- [26] X. Cui, et al., Surface modification of neural recording electrodes with conducting polymer/biomolecule blends, *J. Biomed. Mater. Res.* 56 (2001) 261–272.
- [27] X. Cui, D.C. Martin, Electrochemical deposition and characterization of poly (3, 4-ethylenedioxythiophene) on neural microelectrode arrays, *Sensors Actuators B Chem.* 89 (2003) 92–102.
- [28] X.T. Cui, D.D. Zhou, Poly (3, 4-ethylenedioxythiophene) for chronic neural stimulation, *IEEE Trans. Neural Syst. Rehabil. Eng.* 15 (2007) 502–508.
- [29] J. Albuquerque, et al., A simple method to estimate the oxidation state of polyanilines, *Synth. Met.* 113 (2000) 19–22.
- [30] N.V. Blinova, J. Stejskal, M. Trchová, J. Prokeš, Control of polyaniline conductivity and contact angles by partial protonation, *Polym. Int.* 57 (2008) 66–69.
- [31] T. Lindfors, L. Harju, Determination of the protonation constants of electrochemically polymerized poly (aniline) and poly (3,4-ethylenedioxythiophene) films, *Synth. Met.* 158 (2008) 233–241.
- [32] P. Bober, T. Lindfors, M. Pesonen, J. Stejskal, Enhanced pH stability of conducting polyaniline by reprotonation with perfluorooctanesulfonic acid, *Synth. Met.* 178 (2013) 52–55.
- [33] J. Stejskal, R. Gilbert, Polyaniline. Preparation of a conducting polymer (IUPAC technical report), *Pure Appl. Chem.* 74 (2002) 857–867.
- [34] J. Huang, et al., Investigation of the effects of doping and post-deposition treatments on the conductivity, morphology, and work function of poly (3, 4-ethylenedioxythiophene)/poly (styrene sulfonate) films, *Adv. Funct. Mater.* 15 (2005) 290–296.
- [35] F. Louwet, et al., PEDOT/PSS: synthesis, characterization, properties and applications, *Synth. Met.* 135 (2003) 115–117.
- [36] S.J. Wilks, S.M. Richardson-Burns, J.L. Hendricks, D.C. Martin, K.J. Otto, Poly (3, 4-ethylenedioxythiophene) as a micro-neural interface material for electrostimulation, *Front. Neuroeng.* 2 (2009).
- [37] M.R. Abidian, D.C. Martin, Experimental and theoretical characterization of implantable neural microelectrodes modified with conducting polymer nanotubes, *Biomaterials* 29 (2008) 1273–1283.
- [38] K.A. Ludwig, J.D. Uram, J. Yang, D.C. Martin, D.R. Kipke, Chronic neural recordings using silicon microelectrode arrays electrochemically deposited with a poly (3, 4-ethylenedioxythiophene)(PEDOT) film, *J. Neural Eng.* 3 (2006) 59.
- [39] T. Nyberg, A. Shimada, K. Torimitsu, Ion conducting polymer microelectrodes for interfacing with neural networks, *J. Neurosci. Methods* 160 (2007) 16–25.
- [40] Y. Furukawa, A. Shimada, K. Kato, H. Iwata, K. Torimitsu, Monitoring neural stem differentiation using PEDOT-PSS based MEA, *Biochim. Biophys. Acta Gen. Subj.* 1830 (2013) 4329–4333.
- [41] M.H. Bolin, et al., Nano-fiber scaffold electrodes based on PEDOT for cell stimulation, *Sensors Actuators B Chem.* 142 (2009) 451–456.
- [42] N. Srivastava, et al., Neuronal differentiation of embryonic stem cell derived neuronal progenitors can be regulated by stretchable conducting polymers, *Tissue Eng. A* 19 (2013) 1984–1993.
- [43] D. Esrafilzadeh, J.M. Razal, S.E. Moulton, E.M. Stewart, G.G. Wallace, Multifunctional conducting fibres with electrically controlled release of ciprofloxacin, *J. Control. Release* 169 (2013) 313–320.
- [44] L. Jin, et al., A facile approach for the fabrication of core-shell PEDOT nanofiber mats with superior mechanical properties and biocompatibility, *J. Mater. Chem. B* 1 (2013) 1818–1825.
- [45] A. Townsend-Nicholson, S.N. Jayasinghe, Cell electrospinning: a unique biotechnique for encapsulating living organisms for generating active biological microthreads/scaffolds, *Biomacromolecules* 7 (2006) 3364–3369.
- [46] S.N. Jayasinghe, Cell electrospinning: a novel tool for functionalising fibres, scaffolds and membranes with living cells and other advanced materials for regenerative biology and medicine, *Analyst* 138 (2013) 2215–2223.
- [47] C.E. Schmidt, V.R. Shastri, J.P. Vacanti, R. Langer, Stimulation of neurite outgrowth using an electrically conducting polymer, *Proc. Natl. Acad. Sci.* 94 (1997) 8948–8953.
- [48] E. Stewart, et al., Electrical stimulation using conductive polymer polypyrrole promotes differentiation of human neural stem cells: a biocompatible platform for translational neural tissue engineering, *Tissue Eng.* (2014). <http://dx.doi.org/10.1089/ten.tec.2014.0338> [ahead of print].
- [49] B.C. Thompson, et al., Conducting polymers, dual neurotrophins and pulsed electrical stimulation—dramatic effects on neurite outgrowth, *J. Control. Release* 141 (2010) 161–167.
- [50] J. Xie, et al., Conductive core-sheath nanofibers and their potential application in neural tissue engineering, *Adv. Funct. Mater.* 19 (2009) 2312–2318.
- [51] J. Serra Moreno, M.G. Sabbieti, D. Agas, L. Marchetti, S. Panero, Polysaccharides immobilized in polypyrrole matrices are able to induce osteogenic differentiation in mouse mesenchymal stem cells, *J. Tissue Eng. Regen. Med.* 8 (2012) 989–999.
- [52] J.-W. Lee, F. Serna, J. Nickels, C.E. Schmidt, Carboxylic acid-functionalized conductive polypyrrole as a bioactive platform for cell adhesion, *Biomacromolecules* 7 (2006) 1692–1695.
- [53] H.-K. Song, B. Toste, K. Ahmann, D. Hoffman-Kim, G. Palmore, Micropatterns of positive guidance cues anchored to polypyrrole doped with polyglutamic acid: a new platform for characterizing neurite extension in complex environments, *Biomaterials* 27 (2006) 473–484.
- [54] D.H. Kim, M. Abidian, D.C. Martin, Conducting polymers grown in hydrogel scaffolds coated on neural prosthetic devices, *J. Biomed. Mater. Res. A* 71 (2004) 577–585.
- [55] D. Cheng, H. Xia, H.S. Chan, Synthesis and characterization of surface-functionalized conducting polyaniline-chitosan nanocomposite, *J. Nanosci. Nanotechnol.* 5 (2005) 466–473.
- [56] M. Gizdavic-Nikolaidis, S. Ray, J.R. Bennett, A.J. Easteal, R.P. Cooney, Electrospun functionalized polyaniline copolymer-based nanofibers with potential application in tissue engineering, *Macromol. Biosci.* 10 (2010) 1424–1431.
- [57] M. Li, Y. Guo, Y. Wei, A.G. MacDiarmid, P.I. Lelkes, Electrospinning polyaniline-contained gelatin nanofibers for tissue engineering applications, *Biomaterials* 27 (2006) 2705–2715.
- [58] T. Sergeeva, N. Lavrik, S. Piletsky, A. Rachkov, A. El'Skaya, Polyaniline label-based conductometric sensor for IgG detection, *Sensors Actuators B Chem.* 34 (1996) 283–288.
- [59] M. Tahhan, V.-T. Truong, G.M. Spinks, G.G. Wallace, Carbon nanotube and polyaniline composite actuators*, *Smart Mater. Struct.* 12 (2003) 626.
- [60] G.M. Spinks, B. Xi, V.-T. Truong, G.G. Wallace, Actuation behaviour of layered composites of polyaniline, carbon nanotubes and polypyrrole, *Synth. Met.* 151 (2005) 85–91.
- [61] G.M. Spinks, V. Mottaghtalab, M. Bahrami-Samani, P.G. Whitten, G.G. Wallace, Carbon-nanotube-reinforced polyaniline fibers for high-strength artificial muscles, *Adv. Mater.* 18 (2006) 637–640.
- [62] S.M. Richardson-Burns, et al., Polymerization of the conducting polymer poly (3, 4-ethylenedioxythiophene)(PEDOT) around living neural cells, *Biomaterials* 28 (2007) 1539–1552.
- [63] N. Martino, et al., A Polymer Optoelectronic Interface Restores Light Sensitivity in Blind Rat Retinas, 2013.
- [64] M. Manceau, A. Rivaton, J.-L. Gardette, S. Guillerez, N. Lemaître, The mechanism of photo- and thermooxidation of poly (3-hexylthiophene)(P3HT) reconsidered, *Polym. Degrad. Stab.* 94 (2009) 898–907.
- [65] R. Rodrigues, Q. Ferreira, A.L. Mendonça, J. Morgado, Template role of polyhexylthiophene nanowires on efficient bilayer photovoltaic cells, *Synth. Met.* 190 (2014) 72–78.
- [66] G. Brotas, et al., Synthesis, characterization, and applications in photovoltaic cells of oxetane-functionalized P3HT derivatives, *J. Polym. Sci. A Polym. Chem.* 52 (2014) 652–663.
- [67] G. Brotas, J. Farinhas, Q. Ferreira, J. Morgado, A. Charas, Nanostructured layers of a new cross-linkable poly (3-hexylthiophene) in organic photovoltaic cells, *Synth. Met.* 162 (2012) 2052–2058.
- [68] N. Martino, D. Ghezzi, F. Benfenati, G. Lanzani, M.R. Antognazza, Organic semiconductors for artificial vision, *J. Mater. Chem. B* 1 (2013) 3768–3780.
- [69] D. Ghezzi, et al., A hybrid bioorganic interface for neuronal photoactivation, *Nat. Commun.* 2 (2011) 166.
- [70] R.F.A. Rodrigues, A. Charas, J. Morgado, A.N. Maçanita, Self-organization and excited-state dynamics of a fluorene-bithiophene copolymer (F8T2) in solution, *Macromolecules* 43 (2009) 765–771.

- [71] G. Bernardo, et al., Synergistic effect on the efficiency of polymer light-emitting diodes upon blending of two green-emitting polymers, *J. Appl. Phys.* 108 (2010) 014503.
- [72] Z. Liu, H. Li, Z. Qiu, S.L. Zhang, Z.B. Zhang, SMALL-hysteresis thin-film transistors achieved by facile dip-coating of nanotube/polymer composite, *Adv. Mater.* 24 (2012) 3633–3638.
- [73] J. Jo, et al., Effect of photo-and thermo-oxidative degradation on the performance of hybrid photovoltaic cells with a fluorene-based copolymer and nanocrystalline TiO₂, *J. Mater. Chem.* 18 (2008) 654–659.
- [74] J. Farinhas, et al., Nanostructured donor/acceptor interfaces in photovoltaic cells using columnar-grain films of a cross-linked poly (fluorene-alt-bithiophene), *J. Mater. Chem.* 21 (2011) 12511–12519.
- [75] Z.-S. Kim, S.C. Lim, S.H. Kim, Y.S. Yang, D.-H. Hwang, Biotin-functionalized semiconducting polymer in an organic field effect transistor and application as a biosensor, *Sensors* 12 (2012) 11238–11248.
- [76] M. Ates, T. Karazehir, A.S. Sarac, Conducting polymers and their applications, *Curr. Phys. Chem.* 2 (2012) 224–240.
- [77] Z. Matharu, S.K. Arya, S. Singh, V. Gupta, B. Malhotra, Langmuir–Blodgett film based on MEH-PPV for cholesterol biosensor, *Anal. Chim. Acta* 634 (2009) 243–249.
- [78] Van den Bogaert, R. (Google Patents, 2005).
- [79] L.H. Jimison, et al., Measurement of barrier tissue integrity with an organic electrochemical transistor, *Adv. Mater.* 24 (2012) 5919–5923.
- [80] P.A. Levermore, R. Jin, X. Wang, J.C. de Mello, D.D. Bradley, Organic light-emitting diodes based on poly (9, 9-dioctylfluorene-co-bithiophene) (F8T2), *Adv. Funct. Mater.* 19 (2009) 950–957.
- [81] R. Donato, et al., Differential development of neuronal physiological responsiveness in two human neural stem cell lines, *BMC Neurosci.* 8 (2007) 36.
- [82] E. Stavrinidou, et al., Direct measurement of ion mobility in a conducting polymer, *Adv. Mater.* 25 (2013) 4488–4493.
- [83] R. Hoffrogge, et al., 2-DE proteome analysis of a proliferating and differentiating human neuronal stem cell line (ReNcell VM), *Proteomics* 6 (2006) 1833–1847.
- [84] W. Strober, Trypan blue exclusion test of cell viability, *Curr. Protoc. Immunol.* A 3B. 1-A. 3B. 2 (2001).
- [85] S. Casarosa, J. Zasso, L. Conti, Systems for ex-vivo Isolation and Culturing of Neural Stem Cells, 2013.
- [86] J.C. Conover, R.Q. Notti, The neural stem cell niche, *Cell Tissue Res.* 331 (2008) 211–224.
- [87] P. Hall, J. Lathia, M. Caldwell, Laminin enhances the growth of human neural stem cells in defined culture media, *BMC Neurosci.* 9 (2008) 71.
- [88] M. Lampin, R. Warocquier-Clérout, C. Legris, M. Degrange, M. Sigot-Luizard, Correlation between substratum roughness and wettability, cell adhesion, and cell migration, *J. Biomed. Mater. Res.* 36 (1997) 99–108.
- [89] A. Thapa, T.J. Webster, K.M. Haberstroh, Polymers with nano-dimensional surface features enhance bladder smooth muscle cell adhesion, *J. Biomed. Mater. Res.* A 67 (2003) 1374–1383.
- [90] A.-S. Andersson, et al., Nanoscale features influence epithelial cell morphology and cytokine production, *Biomaterials* 24 (2003) 3427–3436.
- [91] F. Yang, C. Xu, M. Kotaki, S. Wang, S. Ramakrishna, Characterization of neural stem cells on electrospun poly (L-lactic acid) nanofibrous scaffold, *J. Biomater. Sci. Polym. Ed.* 15 (2004) 1483–1497.
- [92] Q. Ferreira, G. Bernardo, A. Charas, L.S. Alcácer, J. Morgado, Polymer light-emitting diode interlayers' formation studied by current-sensing atomic force microscopy and scaling laws, *J. Phys. Chem. C* 114 (2009) 572–579.
- [93] C. Ionescu-Zanetti, A. Mechler, S.A. Carter, R. Lal, Semiconductive polymer blends: correlating structure with transport properties at the nanoscale, *Adv. Mater.* 16 (2004) 385–389.
- [94] X. Li, J. Kolega, Effects of direct current electric fields on cell migration and actin filament distribution in bovine vascular endothelial cells, *J. Vasc. Res.* 39 (2002) 391–404.
- [95] A.Y. Chan, et al., EGF stimulates an increase in actin nucleation and filament number at the leading edge of the lamellipod in mammary adenocarcinoma cells, *J. Cell Sci.* 111 (1998) 199–211.
- [96] J. Settleman, Tension precedes commitment—even for a stem cell, *Mol. Cell* 14 (2004) 148–150.
- [97] R. McBeath, D.M. Pirone, C.M. Nelson, K. Bhadriraju, C.S. Chen, Cell shape, cytoskeletal tension, and RhoA regulate stem cell lineage commitment, *Dev. Cell* 6 (2004) 483–495.
- [98] A.M. Rajnicek, L.E. Foubister, C.D. McCaig, Temporally and spatially coordinated roles for Rho, Rac, Cdc42 and their effectors in growth cone guidance by a physiological electric field, *J. Cell Sci.* 119 (2006) 1723–1735.
- [99] M.D. Treiser, et al., Cytoskeleton-based forecasting of stem cell lineage fates, *Proc. Natl. Acad. Sci.* 107 (2010) 610–615.
- [100] G. Thirivikraman, G. Madras, B. Basu, Intermittent electrical stimuli for guidance of human mesenchymal stem cell lineage commitment towards neural-like cells on electroconductive substrates, *Biomaterials* 35 (2014) 6219–6235.
- [101] X. Yao, R. Peng, J. Ding, Effects of aspect ratios of stem cells on lineage commitments with and without induction media, *Biomaterials* 34 (2013) 930–939.
- [102] Y.-J. Chang, C.-J. Tsai, F.-G. Tseng, T.-J. Chen, T.-W. Wang, Micropatterned stretching system for the investigation of mechanical tension on neural stem cells behavior, *Nanomed.: Nanotechnol., Biol. Med.* 9 (2013) 345–355.
- [103] M.R. Cho, H.S. Thatte, R.C. Lee, D. Golan, Reorganization of microfilament structure induced by ac electric fields, *FASEB J.* 10 (1996) 1552–1558.
- [104] I. Titushkin, M. Cho, Regulation of cell cytoskeleton and membrane mechanics by electric field: role of linker proteins, *Biophys. J.* 96 (2009) 717–728.
- [105] M.R. Cho, H. Thatte, R. Lee, D. Golan, Induced redistribution of cell surface receptors by alternating current electric fields, *FASEB J.* 8 (1994) 771–776.
- [106] M. Zhao, A. Dick, J.V. Forrester, C.D. McCaig, Electric field-directed cell motility involves up-regulated expression and asymmetric redistribution of the epidermal growth factor receptors and is enhanced by fibronectin and laminin, *Mol. Biol. Cell* 10 (1999) 1259–1276.
- [107] M.S. Lord, M. Foss, F. Besenbacher, Influence of nanoscale surface topography on protein adsorption and cellular response, *Nano Today* 5 (2010) 66–78.
- [108] H.T. Nguyen, et al., Electric field stimulation through a substrate influences Schwann cell and extracellular matrix structure, *J. Neural Eng.* 10 (2013) 046011.
- [109] M.R. Cho, A review of electrocoupling mechanisms mediating facilitated wound healing, *IEEE Trans. Plasma Sci.* 30 (2002) 1504–1515.
- [110] M. Zhao, et al., Electrical signals control wound healing through phosphatidylinositol-3-OH kinase-γ and PTEN, *Nature* 442 (2006) 457–460.
- [111] Y. Li, et al., Engineering cell alignment in vitro, *Biotechnol. Adv.* 32 (2013) 347–365.
- [112] M. Théry, Micropatterning as a tool to decipher cell morphogenesis and functions, *J. Cell Sci.* 123 (2010) 4201–4213.
- [113] J.M. Corey, E.L. Feldman, Substrate patterning: an emerging technology for the study of neuronal behavior, *Exp. Neurol.* 184 (2003) 89–96.
- [114] M. Nikkha, F. Edalat, S. Manoucheri, A. Khademhosseini, Engineering microscale topographies to control the cell–substrate interface, *Biomaterials* 33 (2012) 5230–5246.
- [115] L. Yao, A. Pandit, S. Yao, C.D. McCaig, Electric field-guided neuron migration: a novel approach in neurogenesis, *Tissue Eng. B Rev.* 17 (2011) 143–153.
- [116] M. Arocena, M. Zhao, J.M. Collinson, B. Song, A time-lapse and quantitative modelling analysis of neural stem cell motion in the absence of directional cues and in electric fields, *J. Neurosci. Res.* 88 (2010) 3267–3274.
- [117] C.D. McCaig, A.M. Rajnicek, B. Song, M. Zhao, Controlling cell behavior electrically: current views and future potential, *Physiol. Rev.* 85 (2005) 943–978.
- [118] C.D. McCaig, B. Song, A.M. Rajnicek, Electrical dimensions in cell science, *J. Cell Sci.* 122 (2009) 4267–4276.
- [119] J.F. Feng, et al., Guided migration of neural stem cells derived from human embryonic stem cells by an electric field, *Stem Cells* 30 (2012) 349–355.
- [120] A.K. Dubey, S.D. Gupta, B. Basu, Optimization of electrical stimulation parameters for enhanced cell proliferation on biomaterial surfaces, *J. Biomed. Mater. Res. B Appl. Biomater.* 98 (2011) 18–29.
- [121] O. Yanes, et al., Metabolic oxidation regulates embryonic stem cell differentiation, *Nat. Chem. Biol.* 6 (2010) 411–417.
- [122] M. Tsatmali, E.C. Walcott, K.L. Crossin, Newborn neurons acquire high levels of reactive oxygen species and increased mitochondrial proteins upon differentiation from progenitors, *Brain Res.* 1040 (2005) 137–150.
- [123] J. Smith, E. Ladi, M. Mayer-Pröschel, M. Noble, Redox state is a central modulator of the balance between self-renewal and differentiation in a dividing glial precursor cell, *Proc. Natl. Acad. Sci.* 97 (2000) 10032–10037.
- [124] M.J. Higgins, P.J. Molino, Z. Yue, G.G. Wallace, Organic conducting polymer–protein interactions, *Chem. Mater.* 24 (2012) 828–839.
- [125] M.E. Mycielska, M.B. Djamgoz, Cellular mechanisms of direct-current electric field effects: galvanotaxis and metastatic disease, *J. Cell Sci.* 117 (2004) 1631–1639.
- [126] C.A. Ariza, et al., The influence of electric fields on hippocampal neural progenitor cells, *Stem Cell Rev. Rep.* 6 (2010) 585–600.
- [127] L. Hinkle, C. McCaig, K. Robinson, The direction of growth of differentiating neurones and myoblasts from frog embryos in an applied electric field, *J. Physiol.* 314 (1981) 121–135.
- [128] V. Shastri, C. Schmidt, T.-H. Kim, J. Vacanti, R. Langer, *MRS Proceedings*, vol. 414, Cambridge Univ Press, 1995.
- [129] M. Wood, R.K. Willits, Short-duration, DC electrical stimulation increases chick embryo DRG neurite outgrowth, *Bioelectromagnetics* 27 (2006) 328–331.
- [130] Z. Zhang, et al., Electrically conductive biodegradable polymer composite for nerve regeneration: electricity-stimulated neurite outgrowth and axon regeneration, *Artif. Organs* 31 (2007) 13–22.
- [131] Y.-J. Chang, C.-M. Hsu, C.-H. Lin, M.S.-C. Lu, L. Chen, Electrical stimulation promotes nerve growth factor-induced neurite outgrowth and signaling, *Biochim. Biophys. Acta Gen. Subj.* 1830 (2013) 4130–4136.